Shape coexistence and band crossings in ^{174}Pt

J. TM. Goon,[1] D. J. Hartley,[1,*] L. L. Riedinger,[1] M. P. Carpenter,[2] F. G. Kondev,[3] R. V. F. Janssens,[2] K. H. Abu Saleem,[2] I. Ahmad,[2] H. Amro,[4,†] J. A. Cizewski,[5] C. N. Davids,[2] M. Danchev,[1,6] T. L. Khoo,[2] A. Heinz,[2,†] T. Lauritsen,[2] W. C. Ma,[4] G. L. Poli,[2] J. Ressler,[2] W. Reviol,[7] D. Seweryniak,[2] M. B. Smith,[8] I. Wiedenhöver,[2,‡] and Jing-ye Zhang[1]

[1]*Physics Department, University of Tennessee, Knoxville, Tennessee 37996, USA*
[2]*Physics Division, Argonne National Laboratory, Argonne, Illinois 60439, USA*
[3]*Nuclear Engineering Division, Argonne National Laboratory, Argonne, Illinois 60439, USA*
[4]*Physics Department, Mississippi State University, Mississippi State, Mississippi 39762, USA*
[5]*Physics Department, Rutgers University, New Brunswick, New Jersey 08903, USA*
[6]*Faculty of Physics, St. Kliment Ohridski University of Sofia, BG-1164 Sofia, Bulgaria*
[7]*Chemistry Department, Washington University, St. Louis, Missouri 63130, USA*
[8]*TRIUMF, 4004 Wesbrook Mall, Vancouver, British Columbia, Canada V6T 2A3*

(Received 9 March 2004; published 15 July 2004; publisher error corrected 23 July 2004)

High-spin states in ^{174}Pt were populated via the ^{92}Mo(^{84}Sr,$2p$) and ^{92}Mo(^{84}Sr,$2p2n$) reactions. The ground-state band has been extended from $I=14$ to 24 (tentatively 26) and a new side band is observed up to a spin of 21 (tentatively 23). A low-frequency crossing is observed in the latter band at a rotational frequency that is similar to that seen in the ground-state band. The first and second $i_{13/2}$ neutron alignments are also observed in ^{174}Pt. Surprisingly, these crossings occur at approximately the same frequency. Total Routhian surface and cranked shell model calculations are used in an attempt to understand this behavior.

DOI: 10.1103/PhysRevC.70.014309 PACS number(s): 23.20.Lv, 23.60.+e

I. INTRODUCTION

Nuclei near the proton dripline and $Z=82$ have been a unique source of interest with respect to the phenomenon of shape coexistence. Indeed, evidence for triple shape coexistence (prolate, oblate, and spherical) in $^{186}_{82}$Pb [1], $^{179}_{80}$Hg [2,3], and $^{175}_{79}$Au [4] has been presented recently. Examples of shape competition have also been observed further away from the $Z=82$ gap in the Pt, Ir, Os, and Re nuclei (see, for example, Refs. [5–7]). In particular, studies of nonyrast states in ^{176,178,180,182}Pt demonstrate that two coexisting minima (prolate and near-spherical) lie close in energy, with the prolate minimum being yrast for the three heavier nuclei [5]. Theoretical calculations [8] suggest that the prolate minimum is due to the excitation of two (or more) protons across the $Z=82$ gap into $\pi h_{9/2}/f_{7/2}$ and/or $\pi i_{13/2}$ intruder orbitals. Further away from midshell, the near-spherical minimum becomes lower in energy as total Routhian surface (TRS) calculations predict [9,10] weakly deformed, γ-soft minima for the ground states of ^{174,176}Pt. The energy spacings of the yrast bands at low spin in ^{174,176}Pt [9,10] lend support to these suggestions. However, the prolate minimum is low enough in energy that the excited, deformed sequence crosses the near-spherical ground-state structure at low spin ($I\approx 6\hbar$) in ^{172,174,176}Pt [9–11]. Empirical support for this crossing is provided by band-mixing calculations (see, for example, Refs. [5,7,9,11,12]), which also show that the separation between the two minima increases as the neutron number decreases below $N=98$.

The nucleus ^{174}Pt is perhaps one of the clearest examples of this type of band crossing between two minima. However, the effect on the high-spin behavior due to the shape softness was unknown since the highest spin established so far was $I=14$ [9]. In an experiment designed to populate Au nuclei at and beyond the proton dripline [4], high-spin states in ^{174}Pt were observed to be strongly populated. This paper focuses on the results from the ^{174}Pt channel, where the ground-state band was extended to a spin of $I=(26)$ and a side band was clearly established as well. In addition to confirming the low-spin crossing in the ground-state band, there is evidence to suggest that a similar crossing occurs in the side band. An unusual occurrence is also seen, where the first and second $i_{13/2}$ neutron alignments are observed at nearly the same frequency. This may also be the result of the interplay between competing minima with different deformation.

II. EXPERIMENTAL DETAILS

As stated above, the neutron-deficient ^{174}Pt nucleus was produced in an experiment designed to identify excited states in some of the lightest Au nuclei [4]. Beams of 380 and 385 MeV ^{84}Sr ions from the ATLAS superconducting linear accelerator at the Argonne National Laboratory (ANL) were used to bombard ^{92,94}Mo self-supporting targets. The targets that were used were isotopically enriched and ≈ 0.7 mg/cm^2 thick. Excited states in ^{174}Pt were populated via the $2p$ and $2p2n$ evaporation channels, respectively. Prompt γ rays emitted by the recoiling nuclei were detected using 101 Compton-suppressed Ge detectors in the Gammasphere array [13]. The recoils were then passed through the Fragment

*Present address: Department of Physics, United States Naval Academy, Annapolis, MD 21402.
†Present address: Wright Nuclear Structure Laboratory, Yale University, New Haven, CT 06520.
‡Present address: Department of Physics, Florida State University, Tallahassee, FL 32306.

Mass Analyzer (FMA) [14] and were dispersed according to their mass/charge (M/Q) ratio. Time-of-flight and M/Q information of the recoiling nuclei were provided by a position-sensitive parallel grid avalanche counter (PGAC), which was located at the focal plane of the FMA.

The recoiling nuclei were implanted into a 40×40 mm^2, $\approx$60-μm-thick double-sided silicon strip detector (DSSD) located approximately 40 cm behind the PGAC. All events recorded by the DSSD were time stamped by a 47-bit, 1-MHz clock. This information was used to identify recoils and the corresponding α particles emitted by these nuclei. The detected α particles were correlated with γ rays observed at the target position. This technique is known as recoil decay tagging (RDT) [15–17] and allows for the association of γ transitions with the characteristic α-decay energies of the parent nuclei.

The γ-ray data were sorted into γ-coincidence histograms with associated α and/or $A=174$ mass requirements. The γ-ray energies were corrected for Doppler shifts as γ-ray emission occurred while the recoils were in flight ($v/c=0.045$). To select transitions in ^{174}Pt from all other recoils, a matrix of γ rays correlated with the characteristic α-decay line of 6040(5) keV [18,19] was created. In addition, a coincidence cube was sorted, where transitions were restricted to $A=174$ recoils. This provided greater statistics and allowed for a significant extension of the ^{174}Pt decay scheme. The histograms were analyzed with the RADWARE [20] software package. A search for possible α-decay fine structure decaying from ^{174}Pt was performed; however, only the 6040 keV decay could be confidently associated with this nucleus.

III. EXPERIMENTAL RESULTS

Excited states in ^{174}Pt have been previously studied by Dracoulis *et al.* [9]. These authors identified the ground-state band up to spin 14 and observed additional excited states at (1276), 1777, 1796, and 2061 keV. The new level scheme based upon the present study is shown in Fig. 1, where one can see the ground-state band extended from spin 14 to 24 (tentatively 26). Furthermore, a new sideband is now established on top of the 1777 keV state, and is now observed up to $I=21$ (tentatively 23). The (1276) and 1796 keV levels reported in Ref. [9] could not be confirmed.

Figure 2(a) displays a spectrum of the ground-state band (band 1). It was obtained by summing all the combinations of double coincidence gates for transitions above $I=8$ with the transitions below this state. The ordering of the levels above the 14^+ state is based on the measured intensities of the γ rays, which are summarized in Table I. The spin assignment of these new levels must be regarded as tentative at this time. Measurement of the γ-ray angular distributions was found to be nearly isotropic for all transitions. This may be due to the deorientation of ions when recoiling in the vacuum [21]. It is assumed that normal rotational behavior persists above the 14^+ level and, therefore, all newly placed γ transitions in band 1 are considered as stretched $E2$ transitions.

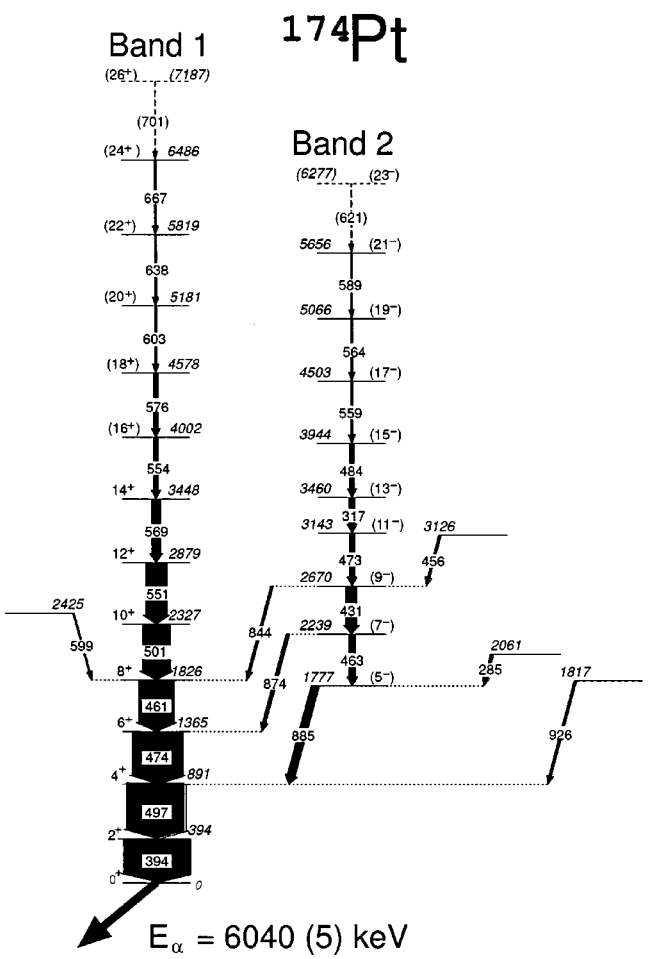

FIG. 1. Level scheme for ^{174}Pt deduced from this work. Tentative spin and parity and placements are given in brackets and dashed lines.

A coincidence spectrum displaying all the γ transitions associated with the new sideband (band 2) is shown in Fig. 2(b). The lowest level observed in band 2 is assumed to be the 1777 keV state. Dracoulis *et al.* [9] suggested that the 431-keV transition feeds the 1365-keV state of band 1. However, using the coincidence cube, it was determined that the 431-keV transition is in coincidence with a 463-keV transition (whose energy is close to the 461 keV ground-state band transition), which feeds the 1777 keV level. Hence, the 431 keV transition is assigned as feeding the resultant 2239 keV state. This ordering is confirmed by the observation of the 885-, 874-, and 844-keV linking transitions from the 1777-, 2239-, and 2670-keV states, respectively (see Fig. 1). Although we favor the placement of the 463-keV transition in band 2, due to its nonrotational behavior in this sequence, it is possible that the 1777 keV state belongs to another structure and the 463-keV transition may be a linking, rather than an inband, transition.

In order to assign spin and parity for band 2, we note that in the neighboring even-even W, Os, and Pt nuclei [10,22–32], the lowest sidebands are consistently found to have negative parity and odd spin. Since the experimental limitations of our data do not allow for firm spin and parity assignments, band 2 is suggested to follow these systematics.

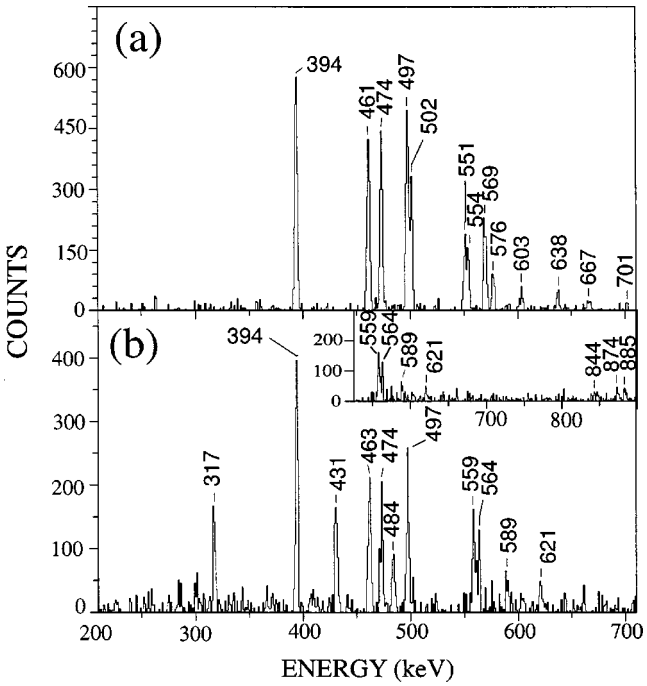

FIG. 2. (a) Spectrum of band 1 where all the combinations of double gates were set between the 394-,497-,474-, and 461-keV transitions with transitions located above the $I=8$ state in band 1. (b) Spectrum for band 2 in which all the combinations of double gates between the 394, 497, and 463 lines with the 317-, 484-, 559-, 564-, and 885-keV lines were added together. The insert in panel (b) displays the high-energy portion of this same spectrum.

Assuming that the prompt transitions have either $E1, M1$ ($M1+E2$), or $E2$ character, $I^{\pi}=3^{-}$ and 5^{-} are two possibilities for the state at 1777 keV. The fact that a transition to the 2^{+} level of the ground-state band was not observed argues against $I^{\pi}=3^{-}$, and hence $I^{\pi}=5^{-}$ is tentatively assigned.

The placement of a relatively low-energy (317 keV) transition at high spin (13) is unusual compared with the systematics of heavier Pt nuclei. However, this γ ray was found in coincidence with the 885-, 874-, and 844-keV interband transitions in band 2. Therefore, this 317-keV transition must be placed above the 2670 keV level. From the efficiency corrected intensities, it was determined that the γ ray feeds the 3143 keV state. Furthermore, similar low-energy γ transitions are found at high spin in the sidebands of ^{170,172}Os [31,32].

A new state at 3126 keV, which feeds the 2670-keV state by the 456-keV transition, is also established; however, no further structure was observed based on this level. The placement of the 285-keV γ transition is in agreement with the previous work [9]. Surprisingly, even though the 285-keV transition is rather strong, no γ rays feeding the 2061-keV state could be confidently identified. In this work, new levels at 1817 and 2425 keV were also established. The 1817 keV state, feeds the 891 keV state of the ground-state band through the 926 keV γ ray, while the 2425 keV level feeds the 8^{+}state via the 599-keV interband transition.

IV. DISCUSSION

In order to discuss the properties of the sequences in ^{174}Pt, the alignment of bands 1 and 2 are plotted versus rotational frequency in Fig. 3. The choice of the Harris parameters, $J_0=25$ MeV^{-1} $\hbar^2$ and $J_1=120$ MeV$^{-3}\hbar^4$, will be addressed below. A sharp gain in alignment is observed at a frequency of 0.24 MeV in band 1. As this interaction occurs at low spin ($I=6$), it is not likely to be the result of a quasiparticle alignment. A similar low-spin perturbation in the ground-state band has been observed in many of the light Os-Pt-Hg-Pb nuclei. Dracoulis *et al.* [9] interpreted this interaction as the crossing of a near-spherical ground-state sequence (g band) by a more deformed vacuum configuration (d band) in the framework of a two-band mixing model. The d band results from a pair of nonaligned quasiprotons scattering from one orbital into a deformation-driving $\pi h_{9/2}/f_{7/2}$ intruder orbital. Therefore, the Harris parameters of the alignment plot were chosen such that the more deformed portion of band 1 has zero alignment. These parameters are consistent with values used in neighboring Pt nuclei [24,25,30].

At higher frequency, another crossing is observed in band 1 at 0.28 MeV with a large gain in alignment. Similar crossings have been observed in bands of the neighboring even-N nuclei; ^{172}Os (0.26 MeV) [32], ^{173}Ir (0.26 MeV) [33], ^{175}Au (0.32 MeV) [4], and ^{176}Pt (0.30 MeV) [10]. These crossings have been consistently interpreted as due to an alignment of $i_{13/2}$ neutrons, which is often referred to as the AB crossing in a cranked shell model (CSM) nomenclature [35]. Therefore, the crossing at 0.28 MeV in the ground-state band of ^{174}Pt is also assigned as the AB alignment. However, the experimental crossing frequency is much higher than the value of 0.22 MeV predicted by CSM calculations assuming $\gamma \leqslant |30°|$, which will be discussed below.

The lowest-lying sideband of even-even nuclei in this region is often associated with a single-phonon octupole vibration [24,31,32,34]. The presence of pairs of orbitals with $\Delta j=\Delta l=3\hbar$ near the Fermi surface contributes to the enhancement of the octupole correlations at low spin. There are neutron and proton orbital pairs ($\nu f_{7/2}, \nu i_{13/2}$ and $\pi f_{7/2}, \pi i_{13/2}$) located near the ^{174}Pt Fermi surface, which satisfy these selection rules. Therefore, it is likely that band 2 is an octupole vibration at lower spins ($I \leqslant 11$). The fact that band 2 has an alignment of $2-3$ $\hbar$ more than the ground-state band (see Fig. 3) for the first three lowest frequencies, is consistent with this interpretation.

In Fig. 3, one may notice an interaction in band 2 at $\hbar\omega=0.23$ MeV that is similar to the low-spin crossing displayed in band 1. This is assuming that the 463 keV γ ray is indeed an inband transition. Following the argument for band 1, it is possible that band 2 begins as an octupole vibration based on the near-spherical ground-state sequence. This structure may then be crossed by an octupole vibrational band based on the more deformed vacuum configuration, which accounts for the interaction at 0.23 MeV. Such a crossing has also been observed in the negative-parity sideband of ^{178}Hg [36].

Band 2 experiences another sharp gain in alignment following the crossing at 0.23 MeV, likely resulting from a change in configuration. After this second crossing in band 2,

TABLE I. Experimental values for γ-ray levels (E_x), spins and parities (J^π), energies (E_γ), and intensities observed in (I_γ) observed in ^{174}Pt.

E_x(keV)	J_i^π	E_γ(keV)[a]	I_γ(rel.)
	Band 1		
393.9	2^+	393.9	1000(20)
891.1	4^+	497.2	857(26)
1364.8	6^+	473.7	758(55)
1826.2	8^+	461.4	515(33)
2327.4	10^+	501.2	416(20)
2878.5	12^+	551.1	319(26)
3447.8	14^+	569.3	126(7)
4001.7	(16^+)	553.9	71(10)
4577.8	(18^+)	576.1	67(5)
5181.2	(20^+)	603.4	33(5)
5819.2	(22^+)	638.0	30(5)
6486.2	(24^+)	667.0	28(4)
(7187.2)	(26^+)	(701.0)	<10
	Band 2		
1776.5	(5^-)	885.4	153(12)
2239.2	(7^-)	462.7	106(17)
2239.2	(7^-)	874.4	51(10)
2670.0	(9^-)	430.8	161(16)
2670.0	(9^-)	844.3	83(6)
3143.2	(11^-)	473.2	92(30)
3459.9	(13^-)	316.7	78(7)
3943.6	(15^-)	483.7	68(9)
4502.5	(17^-)	558.9	37(6)
5066.4	(19^-)	563.9	24(5)
5655.8	(21^-)	589.4	12(6)
(6277.2)	(23^-)	(621.4)	12(6)
	Others		
1817.4		926.3	40(24)
2061.0		284.5	47(7)
2424.8		598.6	42(9)
3125.6		455.6	33(4)

[a]E_γ are accurate to within 0.1-0.3 keV for strong transitions and others to about 0.6 keV.

the sequence likely has the $\nu(i_{13/2,}\, f_{7/2})$ configuration. This interpretation was suggested by de Voigt [26] and has been used to describe similar crossings in sidebands of neighboring ^{174}Os [25], ^{178}Pt [24], and ^{178}Hg [36] nuclei. Following this crossing, band 2 has an additional $\sim 6\hbar$ of alignment as compared with band 1. This is consistent with the suggested change in configuration as the $i_{13/2}$ and $f_{7/2}$ neutrons are associated with $\approx 4\hbar$ and $\approx 2\hbar$ of alignment, respectively. The sharp backbend implies that the interaction strength between the octupole band and the two-quasiparticle configuration is very weak, as is found in ^{168,170,172}Os [31,32]. However, it should be noted that heavier Os and Pt nuclei do not exhibit this phenomenon.

At higher frequency, a third crossing is observed at 0.29 MeV in band 2. The *AB* neutron crossing is Pauli blocked in band 2, because the configuration already involves an $i_{13/2}$ neutron. The next available predicted crossing results from an alignment of a second pair of $i_{13/2}$ neutrons, namely the *BC* crossing. One may notice that this implies that the *BC* crossing is very close to the *AB* crossing (0.28 MeV) in band 1. The small difference between those two neutron crossings is unusual, as normally a frequency difference of approximately 50 keV is observed. See for example, in Fig. 3(b), where the ground-state band and two sidebands involving the $i_{13/2}$ neutron in ^{172}Os [32] are plotted. The *AB* alignment is observed at 0.26 MeV, while the *BC* crossing is found near 0.30 MeV in the sidebands. Since the sidebands in both ^{174}Pt and ^{172}Os display the *BC* crossing near 0.30 MeV, it appears that the *AB* crossing is delayed in the ground-state band of ^{174}Pt.

In order to investigate the nature of this delay, the systematics of the *AB* neutron crossing frequencies found in even-

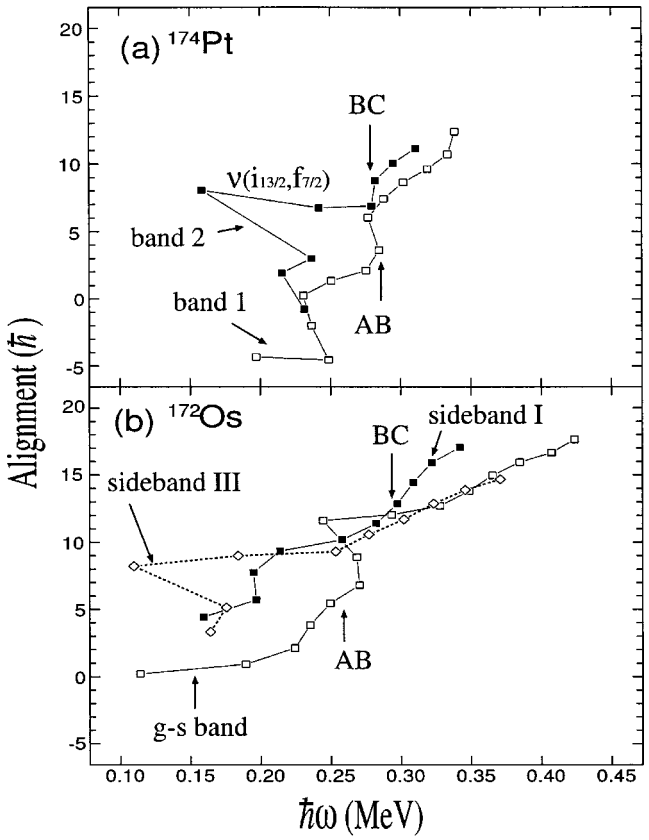

FIG. 3. Alignment as a function of rotational frequency $\hbar\omega$ for (a) bands 1 and 2 in ^{174}Pt and (b) the ground-state and negative-parity sidebands in ^{172}Os. Harris parameters of $\mathcal{J}_0=25\ \hbar^2/\mathrm{MeV}$, $\mathcal{J}_1=120\ \hbar^4/\mathrm{MeV}^3$ and $\mathcal{J}_0=10\ \hbar^2/\mathrm{MeV}$, $\mathcal{J}_1=100\ \hbar^4/\mathrm{MeV}^3$ were used for ^{174}Pt and ^{172}Os, respectively. The notations *AB* and *BC* are discussed in the text.

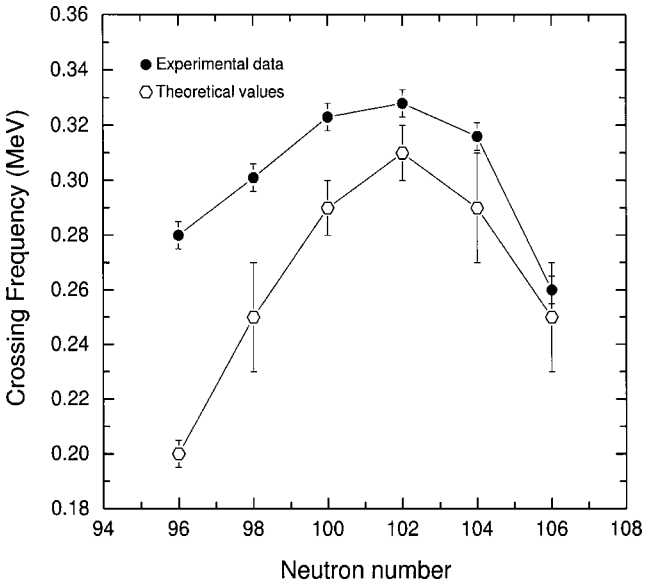

FIG. 4. Crossing frequencies in Pt nuclei ground-state bands for experimental data and theoretical values obtained from the CSM, where parameters are obtained from TRS calculations at $\hbar\omega \approx 0.21$ MeV (denoted by open hexagons). The error bar associated with the theoretical calculations are due to the interaction strength suggested by the CSM.

even Pt nuclei are shown in Fig. 4. Predicted crossing frequencies are obtained from CSM calculations using deformation parameters from TRS calculations [37,38]. The deformation parameters are obtained at a calculated frequency ($\hbar\omega \approx 0.21$ MeV for the Pt nuclei shown in Fig. 4) just below the observed crossing frequency. CSM calculations were then performed to predict the *AB* crossings and the results are compared with experimental values in Fig. 4. In this manner, the calculations are able to reproduce the general trend of the experimental crossings; however, the calculated values are generally smaller than the experimental values. It is possible that the difference in magnitude is due to shape variations following the *AB* alignment. The agreement with the data becomes increasingly worse as the neutron number decreases. It becomes evident that this method may not be the best one for predicting crossing frequencies in the lightest Pt nuclei.

Figure 5 displays the total Routhian surfaces for four frequencies of the ground-state band in ^{174}Pt. At $\hbar\omega \approx 0.21$ MeV [Fig. 5(b)], one can see the complexity of this nucleus as a multiminimum surface is observed. The lowest calculated minimum [labeled as (I) in Fig. 5(b)] has $\beta_2 \approx 0.15$ and $\gamma \approx -25°$, while a second minimum (II) exists with $\beta_2 \approx 0.15$ and $\gamma \approx +15°$, and a third (III) occurs with $\beta_2 \approx 0.19$ and $\gamma \approx -10°$. This latter minimum becomes low-

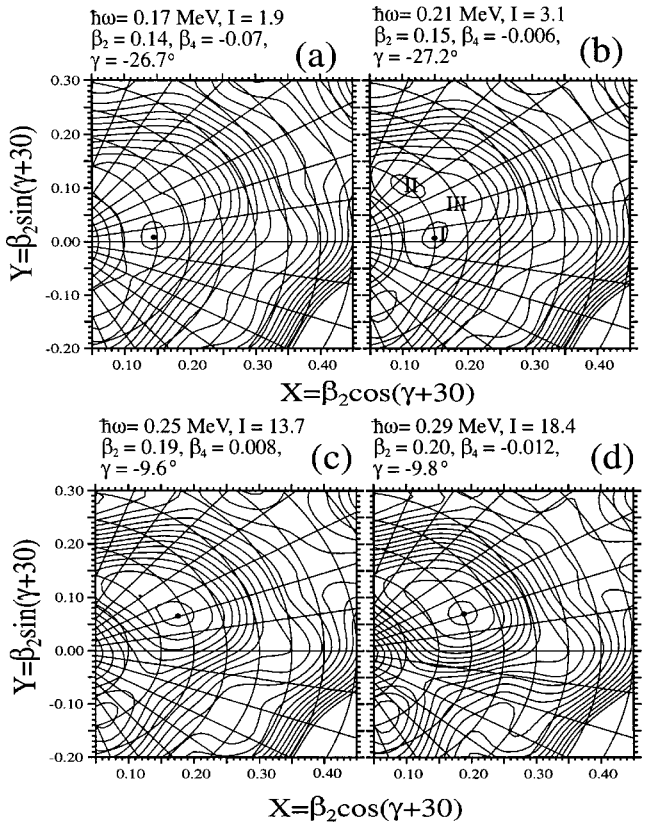

FIG. 5. Total Routhian surfaces at four successive frequencies (denoted in the figure) for the vacuum configuration of ^{174}Pt. Spin and deformation parameters are also given in the figure. Three minima are labeled in panel (b), as discussed in the text.

est at the next highest frequency [Fig. 5(c)], and remains so at $\hbar\omega = 0.29$ MeV [Fig. 5(d)]. The crossing in energy of minimum I and III between $\hbar\omega = 0.21$ and 0.25 MeV agrees well with the experimental data, where a crossing between the near-spherical ground state and deformed prolate band occurs at $\hbar\omega \approx 0.23$ MeV [see Fig. 3(a)]. Based on the gain in spin extracted from the TRS minima, the *AB* alignment has been completed by $\hbar\omega = 0.29$ MeV, stabilizing the shape at $\beta_2 \approx 0.2$ and $\gamma \approx -10°$. It is difficult to fully determine the frequency of the crossing due to the fact that an unperturbed minimum for prolate deformation before the *AB* alignment cannot be isolated because of the interaction from the near-spherical triaxial minima at $\hbar\omega = 0.21$ MeV. From the TRS, we estimate the *AB* crossing frequency to be at $\hbar\omega = 0.26 \pm 0.03$ MeV, which certainly falls within the experimentally observed crossing at $\hbar\omega \approx 0.28$ MeV. Consequently, the TRS calculations provide a rather good description of the observed shape coexistence. In particular, both shape and quasiparticle crossings all occur in a narrow frequency range, i.e., between 0.2 and 0.3 MeV, as observed experimentally. In addition, TRS calculations for band 2 (not shown) predict a crossing near 0.27 MeV, which is in good agreement with the experimental data. While the TRS cannot give a qualitative reason for the apparent delay in the *AB* crossing, it does suggest that mixing between the different shapes and configurations might create a situation where the *AB* crossing appears to be delayed.

V. SUMMARY

The powerful combination of Gammasphere and the FMA allowed for an investigation of shape coexistence and its effect at high spin in ^{174}Pt. The extension of the yrast sequence and the establishment of a sideband revealed several crossings of different types. A shape change in both structures likely causes the crossings observed in both bands near 0.24 MeV. The sideband then changes configuration from an octupole vibration to a two-quasineutron sequence at higher frequencies, and then undergoes the expected *BC* crossing near 0.29 MeV. A delayed *AB* alignment was observed for the ground-state band, which occurs at ≈ 0.28 MeV. An attempt to interpret this crossing with the CSM was determined to be inadequat, as this model is constrained to stable deformation parameters. Thus, it cannot account for any mixing of various shapes at low spin observed in ^{174}Pt. The TRS calculations enhanced the interpretation of these crossings, and it was found that the *AB* alignment is likely delayed by the shape complexity at lower spin.

ACKNOWLEDGMENTS

The authors would like to acknowledge all the help and support provided by the staff and the Physics Support Group of the ATLAS accelerator facility in various phases of the experiment. Thanks also to D. C. Radford and H. Q. Jin for their software support. This work was supported by the U.S. DOE under Contract Nos. DE-FG02-96R40983 (University of Tennessee), W-31-109-ENG-38 (Argonne National Laboratory), DE-FG02-95ER40939 (Mississippi State University), and DE-FG05-88ER40406 (Washington University), as well as the NSF under Grant No. PHY-0300673 (USNA) and PHY-0098800 (Rutgers University).

[1] A. N. Andreyev *et al.*, Nature (London) **405**, 430 (2000).
[2] F. G. Kondev *et al.*, Phys. Lett. B **528**, 221 (2002).
[3] D. G. Jenkins *et al.*, Phys. Rev. C **66**, 011301(R) (2002).
[4] F. G. Kondev *et al.*, Phys. Lett. B **512**, 268 (2001).
[5] P. M. Davidson, G. D. Dracoulis, T. Kibédi, A. P. Byrne, S. S. Anderssen, A. M. Baxter, B. Fabricius, G. J. Lane, and A. E. Stuchbery, Nucl. Phys. **A657**, 219 (1999).
[6] G. D. Dracoulis, B. Fabricius, T. Kibédi, A. M. Baxter, A. P. Byrne, K. P. Lieb, and A. E. Stuchbery, Nucl. Phys. **A534**, 173 (1991).
[7] R. A. Bark, J. Phys. G **17**, 1209 (1991).
[8] R. Bengtsson and W. Nazarewicz, Z. Phys. A **334**, 269 (1989).
[9] G. D. Dracoulis *et al.*, Phys. Rev. C **44**, R1246 (1991).
[10] B. Cederwall *et al.*, Z. Phys. A **337**, 283 (1990).
[11] M. Danchev *et al.*, Phys. Rev. C **67**, 014312 (2003).
[12] G. D. Dracoulis, Phys. Rev. C **49**, 3324 (1994).
[13] I. Y. Lee *et al.*, Nucl. Phys. **A520**, 641c (1990).
[14] C. N. Davids *et al.*, Nucl. Instrum. Methods Phys. Res. B **70**, 358 (1992).
[15] M. P. Carpenter *et al.*, Phys. Rev. Lett. **78**, 3650 (1997).
[16] E. S. Paul *et al.*, Phys. Rev. C **51**, 78 (1995).
[17] R. S. Simon *et al.*, Z. Phys. A **325**, 197 (1986).
[18] Y. A. Akovali, Nucl. Data Sheets **84**, 1 (1998).
[19] J. TM. Goon *et al.* (to be published).
[20] D. C. Radford, Nucl. Instrum. Methods Phys. Res. A **361**, 297 (1995).
[21] G. D. Sprouse, in *Hyperfine Interactions of Radiative Nuclei*, edited by J. Christianesens (Springer-Verlag, Berlin, 1983), Vol. 15.
[22] P. M. Davidson *et al.*, J. Phys. G **12**, L97 (1986).
[23] P. M. Davidson *et al.*, Nucl. Phys. **A568**, 90 (1994).
[24] F. G. Kondev *et al.*, Phys. Rev. C **61**, 044323 (2000).
[25] B. Fabricius *et al.*, Nucl. Phys. **A511**, 345 (1990).
[26] M. J. A. de Voigt *et al.*, Nucl. Phys. **A507**, 472 (1990).
[27] R. M. Lieder *et al.*, Nucl. Phys. **A645**, 465 (1999).
[28] D. G. Popescu *et al.*, Phys. Rev. C **55**, 1175 (1997).
[29] D. T. Joss *et al.*, Nucl. Phys. **A689**, 631 (2001).
[30] M. P. Carpenter *et al.*, Nucl. Phys. **A513**, 125 (1990).
[31] G. D. Dracoulis *et al.*, Nucl. Phys. **A486**, 414 (1988).
[32] R A. Bark *et al.*, Nucl. Phys. **A514**, 503 (1990).
[33] S. Juutinen *et al.*, Nucl. Phys. **A526**, 346 (1991).
[34] G. D. Dracoulis *et al.*, Nucl. Phys. **A383**, 119 (1982).
[35] R. Bengtsson and S. Frauendorf, Nucl. Phys. **A327**, 139 (1979).
[36] F. G. Kondev *et al.*, Phys. Rev. C **61**, 011303(R) (1999).
[37] W. Nazarewicz *et al.*, Nucl. Phys. **A503**, 285 (1989).
[38] R. Wyss *et al.*, Nucl. Phys. **A511**, 324 (1990).